Thermogravimetric study of *n*-alkylammonium-intercalated montmorillonites of different cation exchange capacity

Saheli Ganguly · Kausik Dana · Sankar Ghatak

Abstract Three *n*-alkylammonium salts of varying alkyl chain length were ion exchanged with montmorillonites (MMT) of different cation exchange capacity (CEC). The intercalated MMTs were characterized by thermogravimetry (TG), XRD, FTIR to acquire an insight into the intergallery structural arrangement of the organic alkylammonium cations (AAC). The increment in the intergallery spacing from XRD pattern was correlated with chain length and interlayer arrangement of AAC. Multiple organic mass-loss stages in thermogravimetric analysis indicate two types of anchorage of AAC in intercalated clay. CEC of MMT was found to influence the intergallery confinement and excess adsorption of AAC.

Keywords Montmorillonite · Intercalation · Alkylammonium · Cation exchange capacity · Thermogravimetry

Introduction

The past decade received considerable attention on polymer/inorganic nanocomposites based on the intercalation of polymer chains into organically modified layered silicates (OLS) due to superior physical, mechanical, and thermal properties than conventional mineral-filled composites or unfilled polymers [1–4].

Montmorillonite (MMT) clays intercalated with alkyl ammonium salts are the most significant class of OLS used in polymer nanocomposite. MMT unit cell consists one octahedral Al^{+3}/Mg^{+2} layer sandwiched between two tetrahedral Si^{+4} with variable isomorphic octahedral lattice substitution (Al^{+3} substituted by Mg^{+2}). Stacking of the unit cells occur along c axis. The interlayer positions are occupied by exchangeable cations such as Na^+ or Ca^{+2}, which balance the charge deficiency caused by isomorphous substitution. Intercalation by organic cation expands these layered silicates. The intercalated clay surfaces become organophilic and more compatible with polymer matrix. Apart from nanofiller application in polymers, it can be used as adsorbents for organic pollutants, rheological control agents, in wastewater treatment, as thickening and gelling agent in paints, lubricants, ointments, etc. [5].

The thermal stability of OLS plays a key role in the synthesis and processing of polymer-layered silicate nanocomposites. In-depth understanding of the mechanism of degradation of OLS fillers is needed to develop nanofillers with higher thermal stability. Thermogravimetry is a useful tool to quantify interlayer organic loading, relate the interlayer accumulation of alkylammonium cations (AAC) with the thermal stability of OLS. Degradation studies on alkylammonium and phosphonium-intercalated MMT have been reported [6–15]. Most of these studies were done in nonoxidative atmosphere using High-resolution (HR) thermal analysis. Owing to different heating regimes followed in conventional and HR TG analysis, the peak positions vary in different methods. Also, the earlier workers did not report the effect of cation exchange capacity (CEC) of MMT on thermal stability of the intercalated clay. In this context, it is worthwhile to study the effect of CEC on thermal stability of intercalated MMTs.

In this study, two MMT clays (M1 and M2) with different CEC have been intercalated by three *n*-alkylammonium ions with different alkyl groups, viz., decyl (C_{10}),

S. Ganguly · K. Dana (✉) · S. Ghatak
Advanced Clay and Traditional Ceramics Division,
Central Glass and Ceramic Research Institute, CSIR,
Kolkata 700032, India
e-mail: kdana@cgcri.res.in

hexadecyl (C_{16}), and octadecyl (C_{18}). The intergallery structure and bonding was studied by XRD and FTIR. TG study was done in air atmosphere to study the mass-loss characteristics of the intercalated MMTs. Attempt has been made to relate the thermal stability with structure of intercalated MMT and CEC.

Experimental

Materials

Two montmorillonites, M1 (PGV, Nanocor, USA) and M2 (Neelkanth Minechem, Gujarat, India), were used in this study. M1 was used as received, but M2 was purified, and both were converted to Na^+ form by ion exchange. The intercalates used in this study were decylamine (C_{10}) (95%, FW 157.30), hexadecylamine (C_{16}) (90%, 241.46), and octadecylamine (C_{18}) (97%, 269.52) (Fig. 1). These were supplied by Sigma–Aldrich. These amines were converted to corresponding onium salt solution (M/100) by adding equivalent amount of (1 N) HCl.

Methods

Purification of clays (for M2)

The 1% clay suspension was prepared by adding 100 g of clay in 10 L water. Dil. NaOH was added to adjust pH $\sim$ 7. The suspension was centrifuged at 4,100 g for 5 min, and the supernatant was converted to Na-MMT by ion exchange with Amberlite 120H in Na^+ form. The purified material was dried under vacuum at 75 °C and used in this study.

CEC of M1, M2 was determined by titration with EDTA-complexometric method [16] and were found to be 88 and 62 cmol kg^{-1} of clay, respectively.

Preparation of intercalates of n-alkylammonium salts

One gram of clay was dispersed in 250 mL deionised water and ultrasonicated (0.5 W cm^{-2}) for 60 min at temperature
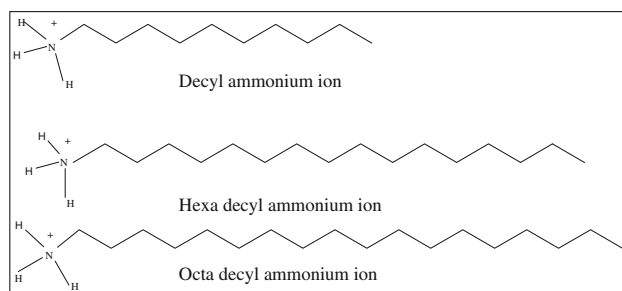

Fig. 1 Structure of intercalates

$\sim$ 70–80 °C. Then the suspension was stirred on a hot plate set at $\sim$ 70–80 °C. Two hundred milliliters intercalant solution (M/100) was added dropwise into this suspension. After addition of intercalant, it was kept under constant stirring at $\sim$ 70–80 °C for 1 h. The reaction mixture was kept overnight for settling. The supernatant water with excess surfactant was decanted, and the flock was redispersed in water. The process was repeated for three times. Then it was filtered under suction and washed with 2,000 mL hot water. The collected product was dried at 70 °C in vacuum drier for $\sim$ 24 h. The dried product was ground in an agate mortar pestle and kept in sealed glass bottles.

X-ray diffraction

The studies on basal spacing of MMT and intercalated MMT were done in XPERT-PRO (PANALYTICAL) diffractometer system. The system was operated at 30 mA, 40 kV between 2.0 and 10.0 (2θ) at a step of 0.05.

Thermogravimetry

TG-DTG analyses of the samples were obtained using instrument NETZSCH STA 409 C. The system was operated at a heating rate 10 °C min^{-1} from 40 up to 1,050 °C in presence of air with $\sim$ 12 mg sample in alumina crucible.

Results and discussion

X-ray diffraction analysis

Understanding of intercalated clay structure is essential for correlating it with its thermal stability. Intergallery arrangement of AACs can be elucidated by X-ray diffraction analysis. Experimental MMTs (M1, M2) showed $d_{001} \sim 1.25$ nm, which is observed in Na^+ MMTs [17].The smectite group of minerals shows variable integral series of basal spacing (d_{001}) which is dependent upon the size of exchangeable cation and on the degree of hydration of the cation.

Intercalation by ion exchange with the AAC increases basal spacing (d_{001}) of experimental MMT clays. Among the three intercalants, C_{16}- and C_{18}-intercalated clay showed the highest $d_{001} = 2.3$ nm (Figs. 2, 3). The increase in d_{001} is due to removal of smaller hydrated interlayer cation by bulky alkyl ammonium salt by ion exchange reaction (Figs. 2, 3). C_{10}-intercalated clay shows a sharp peak, whereas for C_{16}- and C_{18}-intercalated clay showed broadness and diffuseness in XRD peak. The nonintegral series of the *00l* reflections in longer chain salts
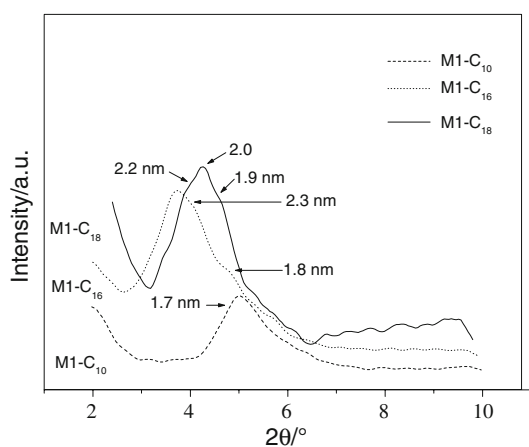
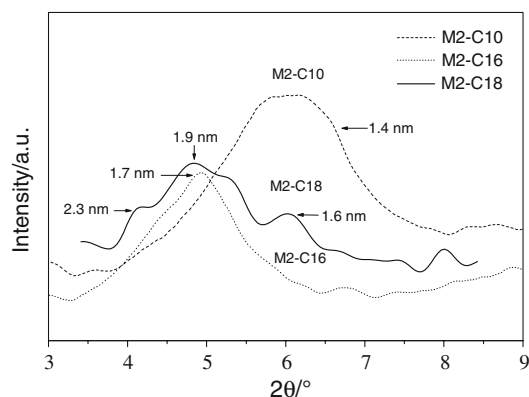**Fig. 2** XRD plots of intercalated-M1 with different AACs

Fig. 3 XRD plots of intercalated-M2 with different AACs

establishes coexistence of different interlayers. Superposition of reflections corresponding to this different interlayer distances created the wide and diffused peak, which suggests coexistence of different intergallery arrangements of AAC. The XRD results depict that increment in basal spacing as well as interlayer arrangement of AAC are mainly guided by two factors, viz., layer charge/CEC of the source clay and chain length of the alkyl group of AAC.

Effect of chain length of AAC

The gallery height "Δ" (Δ = thickness of organic AAC layer sandwiched between two clay layers) was calculated (Table 1) by subtracting the average thickness of one MMT layer (0.96 nm) from d_{001}. The van der Waals thickness of a methyl group is ~ 0.4 nm [17–20]. The Δ value of M2-C_{10} was found to be 0.45 nm, which leaves no option except that the chains lie flat along the clay flake surfaces in monolayers with the planes of the zigzag carbon chains parallel to the plane of clay. $\Delta = 0.6$–0.8 nm predicts a bilayer arrangement of chains in M1-C_{10}, M1-C_{16}, M2-C_{16} because the amount of increment is nearly double the monolayer spacing of 0.3–0.4 nm. Δ value of 1.1–1.2 nm in M1-C_{16}, M1-C_{18}, M2-C_{18} suggests the interlayer *n*-alkyl chains stand more erect, tilted at an angle with the clay surface and begin to slip over one another. In this study, it is found that the overall, homogeneous layer arrangement (monolayer/bilayer) of alkyl chains is preferred by shorter chain (C_{10}), and a heterogeneous mixed (double + paraffinic) layer arrangement is preferred by higher chain lengths(C_{16}, C_{18}) [21, 22].

Effect of CEC of MMT

M1 and M2 are chosen with different cation exchange capacity and hence different layer charge. The heterogeneity in interlayer arrangement develops in M1 for both C_{16} and C_{18}, but in M2, it is seen only in C_{18}. Therefore, as layer charge increases, heterogeneity develops from smaller carbon chain too. Thus, cation exchange capacity, as well as layer charges of the MMT, plays a dominant role in the interlayer arrangements of the AACs.

Apart from information on arrangement of AAC in the intercalated clay from XRD, further details on anchorage of AAC to MMT can be derived from TG.

FTIR analysis

FTIR analysis of the modified MMT samples has been done. The incomplete removal and/or moisture resorption was

Table 1 Correlation between gallery height and interlayer arrangement

Intercalated clay	Raw clay/nm	Clay intercalate/nm	Gallery height (Δ)/nm	Arrangement
M1-C_{10}	1.25	1.7	0.75	Bilayer
M1-C_{16}		1.8, 2.3	0.85, 1.35	Bilayer, paraffinic
M1-C_{18}		1.9, 2.0, 2.2	0.95, 1.05, 1.25	Paraffinic
M2-C_{10}	1.25	1.4	0.45	Monolayer
M2-C_{16}		1.7	0.75	Bilayer
M2-C_{18}		1.6, 1.9, 2.3	0.65, 0.95, 1.35	Paraffinic

Fig. 4 FTIR plots of intercalated-M1 with different AACs

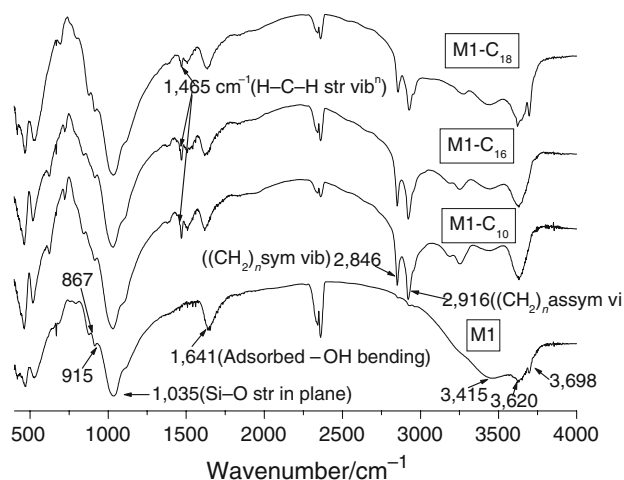Fig. 5 TG plots of intercalated-M1 with different AACs

Fig. 6 TG plots of intercalated-M2 with different AACs

revealed from FTIR spectroscopy (Fig. 4). The IR bands at 3,415 and 1,641 cm^{-1} are $\nu_{\text{-OH (adsorbed)}}$ and $\delta_{\text{-OH (adsorbed)}}$, respectively. The intensity of these bands was reduced to a large extent on intercalation of MMT. This is due to removal of interlayer hydrated cations (and associated hydroxyls) by alkylammonium groups on ion exchange, leading to formation of hydrophobic surface. The intercalated MMT surface populated with bulky alkyl chains makes less space available for adsorption of water molecules.

The characteristic bands at 1,035 and 1,115 cm^{-1} ($\nu_{\text{Si-O}}$), 915 cm^{-1} (δ_{AlAlOH}), 867 cm^{-1} (δ_{AlFeOH}) [22–24] were unaltered on ion exchange with the alkyl ammonium ions. This indicates reversal of the hydrophilic nature of clay surface may not affect the dehydroxylation loss phenomenon.

Thermogravimetric analysis

The TG studies (in air atmosphere) of raw clays (M1 and M2) reveal two major temperature regions of mass loss (Figs. 5, 6). In first step, adsorbed water is lost up to 200 °C. The second step is dehydroxylation of MMT, which occurs between 500 and 800 °C. After intercalation, the intercalated clay shows an additional peak within the temperature region of 200–500 °C due to the decomposition of incorporated organic molecules [6, 7].

Loss of water

At lower temperature (100–200 °C), physically adsorbed moisture is removed. The ease of removal depends on hydration state of interlayer cation in exchange position. The experimental clays were heat-treated at 120 °C to remove adsorbed moisture; therefore, the plots have been drawn from 200 °C. However, incomplete removal and/or moisture resorption was observed from FTIR spectroscopy.
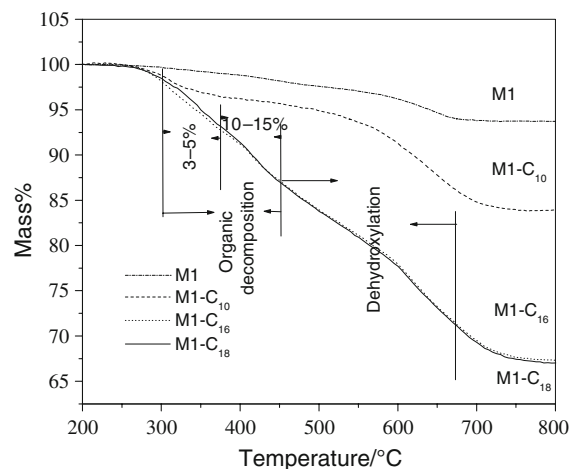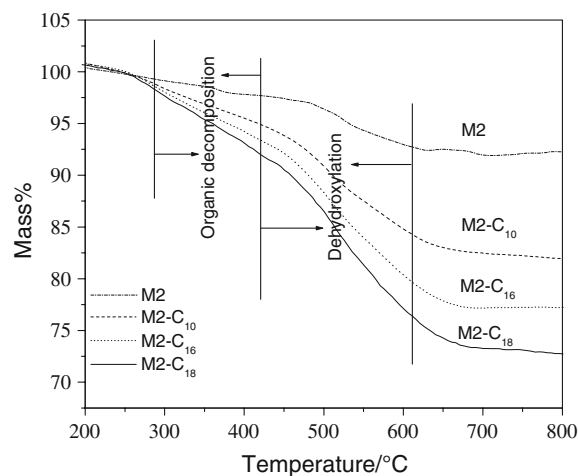
Most MMTs with relatively small amount of iron and magnesium replacing aluminum show an endothermic reaction due to loss of hydroxyl lattice water, beginning gradually at 450–500 °C, ending at about 750 °C [13]. M1 showed peak dehydroxylation temperature near 650 °C, but high octahedral substitution of aluminum by iron in M2 (Figs. 7, 8) resulted in lower peak temperature (500–530 °C). In the experimental MMTs, this loss partly overlapped with organic mass loss in the TG plots (Figs. 5, 6). DTG plots, however, reveal different regions of mass loss. For intercalated clays of M1 and M2, the nature of DTG plots is nearly unaltered. The dehydroxylation region is also distinguishable from the organic mass-loss region. In general, intercalation was found to affect mass loss in
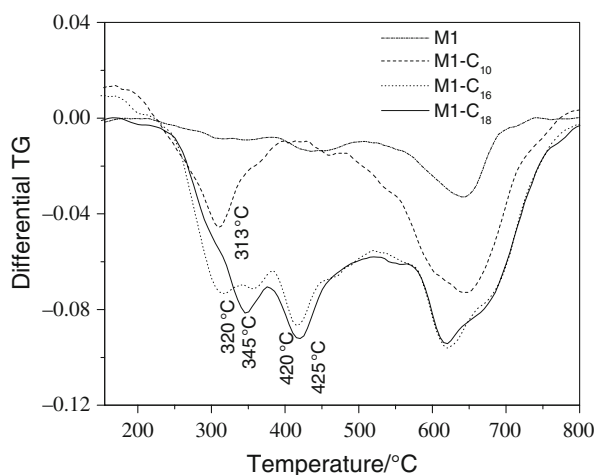
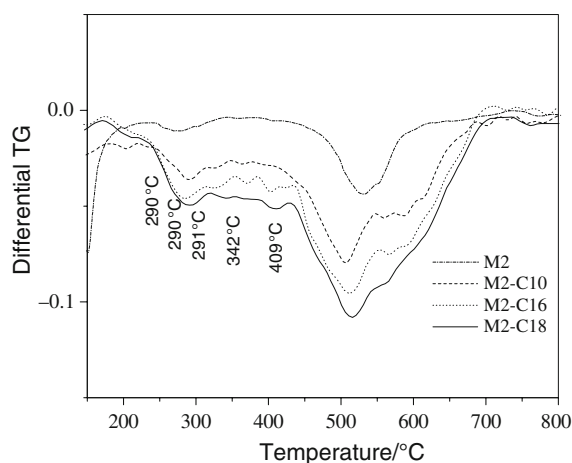Fig. 7 DTG plots of intercalated-M1 with different AACs

Fig. 8 DTG plots of intercalated-M2 with different AACs

this region only marginally, which is also supported by IR analysis. This may be due the fact that inner-layer hydroxyl bonding is not affected by intercalation.

Loss of organics

DTG plots (Figs. 7, 8) clearly show that the multistep thermal transitions occurred in C$_{16}$- and C$_{18}$-intercalated MMTs at two temperature region viz (300–350 and 400–425 °C). This indicates two types of anchorage of the long-chain surfactant molecules in the organo clays. The mass loss associated with the first peak (300–350 °C) is 3–5 mass%, and it indicates that there exists a significant amount of intercalate which is weakly linked to clay surfaces or linked by van der Waals forces with intercalated alkyl chains. While the second (and main) decomposition peak
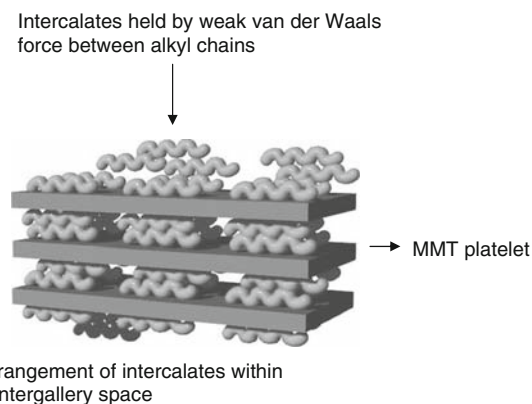

Fig. 9 Schematic representations of two possible types of anchorage of AAC molecules with MMT

(400–425 °C) with mass loss of 10–15 mass% is associated with strongly confined intercalants within the interlayer space [25–27]. Here, the cationic heads (N$^+$) of AAC electro statically bonded to cation exchange sites of MMT which need higher energy to remove from the gallery. A schematic diagram has also been proposed (Fig. 9). Therefore, we can distinguish the peaks in lower temperature region as a desorption peak and the next higher temperature one as main decomposition peak. This excess adsorption is also guided by the two factors, chain length of the AAC and CEC of the source clay.

TG data have been used to measure the amount of intercalation in intercalated clay. The samples were heated at 120 °C for 120 min in air oven prior to TG analysis to remove the adsorbed water. The following calculation was used to quantify organic loading from TG data (200–800 °C) and relate it to exchange capacity (meq/100 g) of MMT.

Calculation of organic content from TG

Let clay show x% mass loss.

Modified clay show y% mass loss.

Let modified clay has n% organic loading. Therefore, its 100 g contains n g organic + $(100 - n)$ g clay.

Now, mass loss from 100 g of modified clay $= n + \{(100 - n)*x\}/100$.

$$y = n + \{(100 - n) * x\}/100$$

$$n = \{100 * (y - x)\}/(100 - x)$$

Now, n g organic is attached to $(100 - n)$ g clay.

Therefore, % organic loading $(z) = (n*100)/(100 - n)$.

Organic milliequivalent/100 g of clay $= \{z/(M.W \text{ of the AAC})*1{,}000\}$

The result for individual clays has been furnished in Table 2.

Table 2 Mass loss at different DTG peak temperatures

Clay	AAC	DTG peak/°C				Mass loss 2 and 3/%	Mass loss 4/%	Organic loading/cmol kg^{-1}	CEC by EDTA method
		1	2	3	4				
M1	C_{10}		313			4		73	88
	C_{16}		320		420	5	10	165	
	C_{18}			345	425	5	10	148	
M2	C_{10}	290						86	62
	C_{16}	290						87	
	C_{18}	291		342	409	Negligible		110	
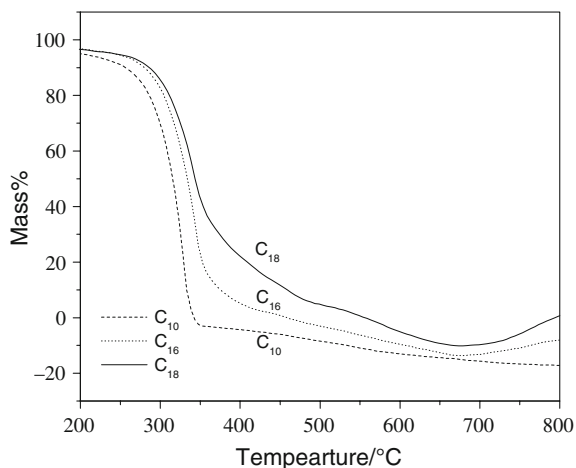
Fig. 10 TG plots of intercalates
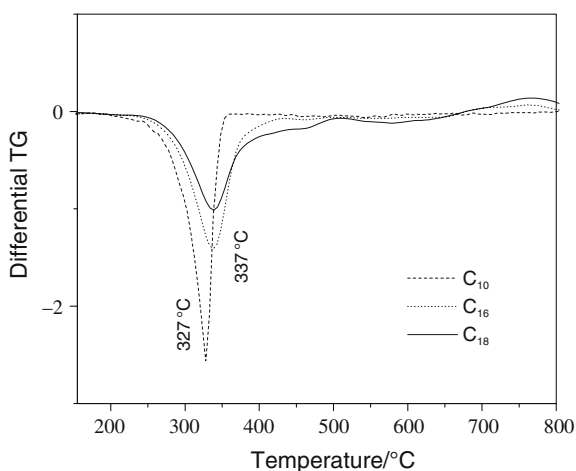
Fig. 11 DTG plots of intercalates

Effect of the chain length

The arrangement of intercalants in the interlayer space also affected the mass-loss curve. The TG (and DTG) analyses of the individual AACs in powder form (Figs. 10, 11) show that C_{10} ammonium salt decomposes at $\sim$327 °C, and C_{16}

and C_{18} ammonium salt decomposes at $\sim$337 °C. In the intercalated clay of long-chain molecule (C_{16} and C_{18} group), the maximum desorption temperature of surfactant at clay surface is nearly the decomposition temperature of individual intercalant. Slight lowering of maximum desorption temperature can be attributed to the catalytic contribution of aluminosilicate surface [8–10]. However, the main decomposition peak is much higher ($\sim$400 °C) than that of individual intercalants (337 °C). This indicates that the longer chain surfactants are arranged in more ordered way within the gallery. Thus, the inferences of XRD, which confined long-chain amines exist in bilayer and paraffin-type layers and are associated more strongly due to van der Waals interaction, are supported by TG-DTG findings. The IR bands in intercalated clays found at 2,916 and 2,846 cm^{-1} are ascribed to asymmetric and symmetric vibration of methylene group of the aliphatic chain. In addition to this, there is also a peak at 1,465 cm^{-1} arising due to H–C–H stretching vibration.

However, the short chain i.e., C_{10}-surfactant-intercalated-clay shows only one sharp decomposition peak in 300–320 °C. This peak seems due to decomposition of adsorbed and intercalated AACs. Both the adsorbed and intercalated salts decompose nearly at the temperature of the individual intercalate in bulk phase. The short-chain AACs are arranged in monolayers or bilayers (in homogeneous phase) within clay galleries. They are less strongly associated as the confined long chain (C_{16} and C_{18} ammonium salts) due to less van der Waal interaction. Therefore, the absence of strongly attached several multi-layer arrangements of the short-chain amine salts in the gallery is the reason for the absence of the decomposition peak in higher temperature zone.

As a consequence of different degree of confinement and anchorage of AACs between clay layers, different organic loading is observed. The high value of organic loading in M1-C_{16}, M1-C_{18}, and M2-C_{18} is due to excess surface adsorption "over CEC". The mass loss associated with the 400–425 °C region closely matches the CEC of the experimental MMTs, while in the 300–350 °C region

presence of excess adsorption of AAC is revealed (Figs. 7, 8). The excess adsorption "over CEC" is prevalent in longer chain AACs due to extensive van der Waals interaction operating between alkyl chains.

Effect of CEC

The organic loss region in TG of the MMTs differs qualitatively for experimental AACs. While M2 (CEC = 62 cmol kg^{-1}) shows only a single-step organic loss, an additional organic loss regime was found in M1 (CEC = 88 cmol kg^{-1}). This low temperature organic mass loss has been linked to weakly anchored AAC molecules. Intercalated M1 contains greater number of alkyl chains at the exchange sites of MMT platelet—which allow greater overlapping of alkyl chains (Fig. 9). Thus higher CEC has lead to increased van der Waals interaction and physical adsorption of AACs on MMT in M1.

Quantitatively, mass loss associated with removal of confined AACs in the exchange position of MMTs was higher in M1 due to high CEC. This is expected, since higher CEC provides greater number of cation exchange sites to which the cationic (N$^+$) head of AACs can attach to.

Lesser confinement of AACs in MMT was observed with lower CEC (M2). Lower decomposition peak temperature (290 °C) in M2 intercalated clay compared to the peak temperature of M1 (310–350 °C) can be explained by lower layer charge in M2 which leads to lesser confinement of the AAC in cation exchange sites of the clay platelets.

Conclusions

Multiple organic mass-loss stages in DTG indicate two types of anchorage of AAC in intercalated clay. Considerable amount of AAC desorbed at lower temperature (300–350 °C) is weakly linked by van der Waals interaction with intercalated alkyl chains or with clay surface. The AAC linked to clay at exchange sites, confined within the intergallery space, is removed at higher temperature (400–425 °C) during heating. The extent of excess adsorption is dependent upon the chain length of AAC and CEC of the clay.

(i) The shorter chain AACs (C$_{10}$) form homogeneous monolayer or bilayer arrangement in interlayer space of MMT. They decompose nearly at the temperature of individual bulk intercalates.

(ii) Longer chain AAC-intercalated clays decompose at much higher temperature than individual AACs due to robust anchorage to clay by strong electrostatic interaction and extensive van der Waals forces.

(iii) Higher CEC MMT shows additional organic loss at low temperature due to desorption of weakly anchored AAC molecules. Low CEC MMTs do not show such desorption peak.

(iv) Mass loss associated with removal of confined AACs in the exchange position of MMTs was higher in M1 due to higher CEC.

(v) Lesser confinement of AACs in MMT was observed with lower CEC.

References

1. Alexandre M, Dubois P. Polymer-layered silicate nanocomposites: preparation, properties and uses of a new class of materials. Mater Sci Eng R. 2000;28:1–63.
2. Sinha Ray S, Okamoto M. Polymer/layered nanocomposites: a review from preparation to processing. Prog Polym Sci. 2003;28:1539–641.
3. Ruiz-Hitzky E, Aranda P, Serratosa JM. Clay organic interactions: organoclay complexes and polymer-clay nanocomposites. In: Auerbach S, Carrado KA, Dutta P, editors. Handbook of layered materials. New York: Marcel Dekker; 2004. p. 91–154. (Chap. 3).
4. Giannelis EP. Polymer layered silicate nanocomposites. Adv Mater. 1996;8:29–35.
5. Bergaya F, Theng BKG, Lagaly G. Handbook of clay science: developments in clay science, vol. 1. Amsterdam: Elsevier Ltd; 2006.
6. Xie W, Gao Z, Pan WP, Hunter D, Singh A, Vaia R. Thermal degradation chemistry of alkyl quaternary ammonium montmorillonite. Chem Mater. 2001;13:2979–90.
7. Xie W, Xie R, Pan WP, Hunter D, Koene B, Tan LS, et al. Thermal stability of quaternary phosphonium modified montmorillonites. Chem Mater. 2002;14:4837–45.
8. Zhu J, Morgan AB, Lamelas FJ, Wilkie CA. Fire properties of polystyrene-clay nanocomposites. Chem Mater. 2001;13:3774–80.
9. Vanderhart DL, Asano A, Gilman JW. Solid state NMR investigation of paramagnetic nylon-6 clay nanocomposites. 2. Measurement of clay dispersion, crystal stratification, and stability of organic modifiers. Chem Mater. 2001;13:3796–809.
10. Fajnor VS, Hlavaty V. Thermal stability of clay/organic intercalation complexes. J Therm Anal Calorim. 2002;67:113–8.
11. Nyden MR, Gilman JW. Molecular dynamics simulations of the thermal degradation of nano confined polypropylene. Comput Theor Polym Sci. 1997;7:191–8.
12. Zidelkheir B, Abdelgoad M. Effect of surfactant agent upon the structure of the montmorillonites: X-ray diffraction and thermal analysis. J Therm Anal Calorim. 2008;94:181–7.
13. Onal M, Sarikaya Y. Thermal analysis of some organo clays. J Therm Anal Calorim. 2008;91:261–5.
14. Xi Y, Zhou Q, Frost R, He H. Thermal stability of octadecyltrimethylammonium bromide modified montmorillonite organoclay. J Colloid Interface Sci. 2007;311:347–53.
15. Avalos F, Ortiz JC, Zitzumbo R, Manchado MAL, Verdejo R, Arroyo M. Phosphonium salt intercalated montmorillonites. Appl Clay Sci. 2009;43:27–32.
16. Mehlich A. Determination of cation- and anion-exchange properties of soils. Soil Sci. 1948;66:429–45.
17. Grim Ralph E. Clay mineralogy. 2nd ed. New York: McGraw Hill; 1968.
18. Favre H, Lagaly G. Organo-bentonites with quaternary alkylammonium ions. Clay Miner. 1991;26:19–32.

19. Lagaly G, Beneke K, Weiss A. Kenyaite—synthesis and properties. Am Miner. 1975;60:642–9.

20. Theng BKG. The chemistry of clay-organic reactions. New York: Wiley; 1974.

21. Yuqin L, Hatsuo I. A differential scanning calorimetry study of the assembly of hexadecylamine molecules in the nanoscale confined space of silicate galleries. Chem Mater. 2002;14:1398–404.

22. Patel HA, Somani RS, Bajaj HC, Jasra RV. Preparation and characterization of phosphonium montmorillonite with enhanced thermal stability. Appl Clay Sci. 2007;35:194–200.

23. Farmer VC. Infrared spectra of minerals. London: Mineralogical Society; 1974.

24. Madejova J. FTIR techniques in clay mineral studies. Vib Spectrosc. 2003;31:1–10.

25. Garcia-Lopez D, Gobernado-Mitre I, Fernandez JF, Merino JC, Pastor JM. Influence of clay modification process in PA6-layered silicate nanocomposite properties. Polymer. 2005;46:2758–65.

26. Xi Y, Martens W, He H, Frost RL. Thermogravimetric analysis of organoclays intercalated with the surfactant octadecyl-trimethylammonium bromide. J Therm Anal Calorim. 2005;81:91–7.

27. Yariv S. The role of charcoal on DTA curves of organo-clay complexes: an overview. Appl Clay Sci. 2004;24:225–36.